Development of an Integrated Model for Selective Metal Laser Sintering

F. Klocke[1] (1), C. Wagner[1], C. Ader[1]
[1]Fraunhofer-Institute of Production Technology IPT, Aachen, Germany
Submitted by F. Klocke (1)

Abstract
Complex physical processes with many single mechanisms, each affecting the other, can be investigated by creating submodels. Submodels enable a better understanding of partial aspects, because fuzzy and not obvious interactions are eliminated. Finally the submodels are merged to an integrated model, representing the base for process simulation, for example. In this paper, the development of an integrated model for Selective Metal Laser Sintering, composed of 4 different submodels, is presented.

From testing and observing it was found that the fusing velocity of powder particles is depending intensely on the maximum process temperature and its semi solid properties. Another important aspect, influencing the process result of metal laser sintering, is oxydation. Oxyde layers repress the sintering and wetting behaviour. Furthermore, the resulting metallic structure is important for the material properties and the quality of the final part.

Facing all this, 4 submodels, e.g. the thermal submodel, the metallurgical submodel, the chemical submodel and the sintering submodel have been generated to describe Selective Metal Laser Sintering. Through this, the sub mechanisms have been specified in a quantitative way. The material behaviour, starting from a single particle to the final laser sintered structure, has been described using a standard cell unit. The modelled material behaviour has been simulated in a FEM-Analysis.

Keywords:
Laser Sintering, Metal Powder Processing, Modelling

1 INTRODUCTION

The objective of this paper is to enhance the know-how on the interaction of physical mechanisms or sub processes in Selective Laser Sintering (SLS). In many cases, research on the technology is done by the empirical investigations on individual materials, gaining expertise with proceeding examinations. Here, the approach of an integrated model, applicable to a greater range of materials – metals and also non-metals – has been made. The model refers to the integrated model of Sun. With regard to special effects of metal processing, it was expanded by metallurgical and chemical sub processes, see figure 1 [1, 2].

The modified model is considered to be helpful in SLS process development, especially when qualifying new metal materials. When an alloy shall be laser sintered, for instance, the question arises, whether it is more suitable to process the powder made from alloy material or to use a powder mixture of the alloying components. Answers can be found from investigations on metallurgical processes, like nucleation or alloying for example. These have an impact on the actual process procedure as well as on the composition of the final structure. Another example can be found in laser sintering of composites – e.g. hard metals - where wetting of solid phases by the liquid is an essential. Therefore surface conditions and chemical reactions – e.g. oxydations – have to be considered by chemical submodels.

The procedure of modelling and sub-modelling started with a detailed process analysis, identifying all influencing factors of SLS, or at least as much as possible from the standard of knowledge. Many works from other places were included [3, 4, 5, 6, 7, 8, 9]. In the next step, topics for submodels were defined. That was predominantly done by process observation and the referring practical experience: all mechanisms that produce or consume energy or that account for mechanical forces were analysed and configurated in five different submodels. By superposing parts of the submodels, a process simulation by FEM was performed.

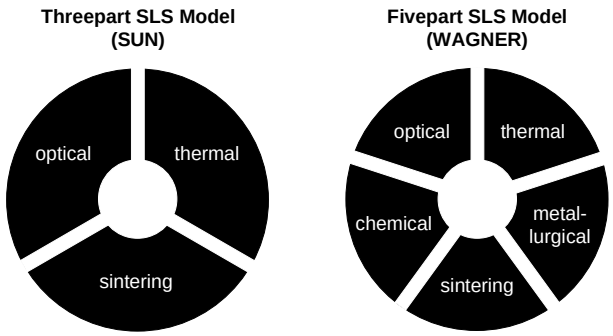

Figure 1: Comparison of the SUN and WAGNER SLS-process model.

2 PROCESS ANALYSIS

Figure 2 gives an overview about the input-output process scheme. The SLS process model, including all submodels, is situated as black box between process input and output parameters.

The first step, before SLS process modelling, was a listing of all input parameters and boundary conditions that can theoretically effect the process result, albeit the quantity of their influence. It was distinguished between

direct and **derived input parameters**: all input parameters that can be modified directly or that are constitutional by materials values were characterised as direct. There are also some essential and helpful input parameters of SLS which depend on two or more direct input parameters; they were characterised as derived input parameters. Examples for the latter can be found in all parameters that are stamped by the powder character: for instance, the absorption coefficient of powder is depending on many different factors. Just like the process procedure itself (transformation from input parameters to output parameters), derived process parameters also have to be modelled.

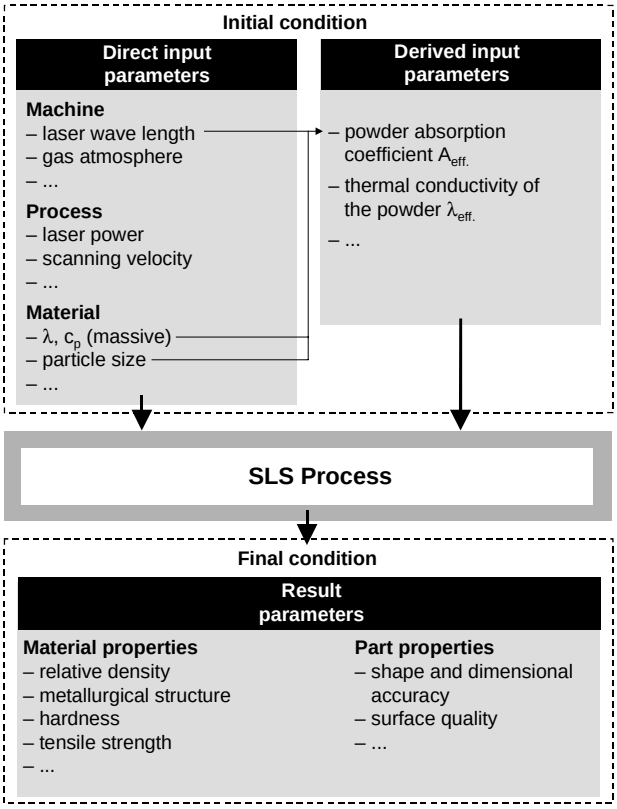

Figure 2: Process scheme of SLS.

2.1 Direct input parameters

In order to get an better overview, the direct input parameters were clustered into machine, process and material based parameters. In Figure 3 a-c, Ishikawa-diagrammes form the input parameter analysis are given.

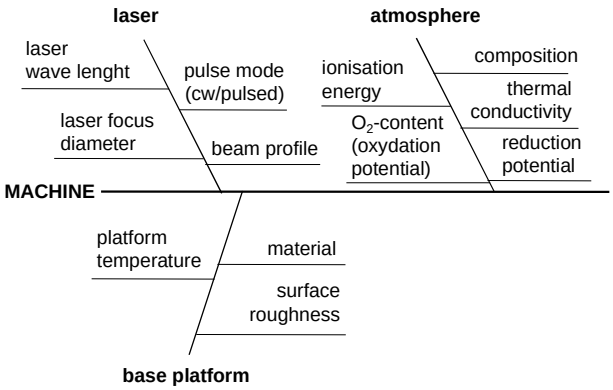

Figure 3a: Machine based input parameters.

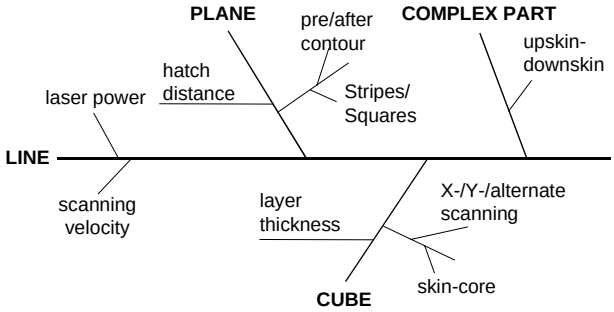

Figure 3b: Process based input parameters.

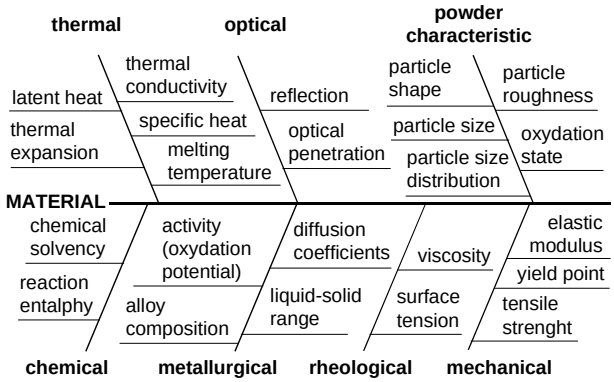

Figure 3c: Material based input parameters.

2.2 Derived input parameters

As mentioned above, derived input parameters are constituted of direct input parameters. Following parameters have been identified [2]:

- powder recoating behaviour/powder flow properties
- bulk density ρ_{bulk}
- powder absorption coefficient $A_{eff.}$
- thermal properties of powder (effective thermal conductivity $\lambda_{eff.}$, effective specific heat $c_{p,\,eff.}$)
- reaction entalphy and intensity
- specific surface energy

2.3 Result parameters

Result parameters are all factors which can be identified in a qualitative way or measured in a quantitative way after the process. By analysing the result parameters, conclusions can be drawn on what happened during the process and cause-and-effect chains can be derived from empirical investigations. In the following paragraphs, parameters are listed only. More detailed descriptions are given in [2].

The output or result parameters have also been clustered: material based properties and part based properties, see figure 2.

3 MODELLING

The laser sintering process can be interpreted as result of superposition and interaction of sub-processes. In the following, the approach of each submodel is described.

3.1 Optical submodel

The basic condition for a physical change within the powder bed is the propagation of a temperature field, induced by laser radiation. Within the optical submodel, the absorption properties of the powder bed surface and the modelling of the heat source are of interest. In discussions of absorption of laser radiation on compact material, like in laser hardening for instance, the laser

wave length, the kind of material, the surface condition and the temperature T are the decisive factors [10]. In the absorption of powder bulks, topological boundary conditions appear additionally. The absorption of metal powders is much higher compared to the compact material. At room temperatures the absorption coefficient A of metal alloy powders amounts between 30 % and 45 % for CO_2-radiation and for an average particle size of about 30 µm. The values of compact, clean and polished metals amounts between 2 % and 8 % for the same wave length. The enhanced absorption of powders is conditioned on the special topology of powder beds and oxyde layers on particle surfaces. The latter can make up to 80 % of the absorptivity, as was found out in investigations [2].

The absorption value of room temperature decreases during the heating in laser sintering until the absorption value of the melt, which is about 11-13 % for steel melts [11]. Further investigations on this topic would allow to derive an empirical function of the kind $A(T, \rho_{rel.})$, where $\rho_{rel.}$ is the actual relative density of the powder bed. However, in the process simulation presented here, the absorption coefficient was put to an averaged value of 20 %.

3.2 Thermal submodel

When modelling the temperature field and its propagation, boundary conditions, an energy balance and heat transport mechanisms have to be defined. Boundary conditions are, for example, all internal and external heat sources. The laser beam can be modelled as surface or volumetric heat source, defining the energy distribution or any movements of the source. Lattice energies and also energies of chemical reactions might be considered. Process simulations of laser hardening or laser welding show some parallels to SLS and can be used to start thermal modelling of laser sintering. However, like in the optical submodel, the big difference of these processes exists in the powder material. The powder bulk requires a special modelling of the thermal material parameters, thermal conductivity λ and specific heat c_p, which depend on temperature T and relative density $\rho_{rel.}$. The specific heat c_p is relatively easy to determine, once the relative density is known: neglecting the thermal capacity of the void fraction, c_p is linearly dependent on $\rho_{rel.}$. The modelling of the thermal conductivity is more complex. It depends mainly on the contact surface of the particles, which itself is a function of the powder characteristic. Many models of heat transfer in powder beds have been drawn in the past, but none is completely applicable on SLS [12]. However, in practical investigations of the coalescence behaviour with two powder grains, it was found out, that the fusion happens “immediately” (in less than 2 ms), when the temperature of the material exceeds the melting temperature $T_{melt.}$ or the liquidus temperature $T_{liq.}$ for alloys respectively [13]. That means also that the contact surface of the particles changes “immediately” at melting. Therefore, the effective thermal conductivity $\lambda_{eff.}$, depending on temperature T, was set simplifying to:

$T < T_{sol.}$: $\lambda_{eff.} \equiv \lambda_{bulk}$

$T_{sol.} < T < T_{liq.}$: $\lambda_{eff.} \equiv \lambda_{bulk} + \frac{T - T_{sol.}}{T_{liq.} - T_{sol.}} \cdot (\lambda_{massive} - \lambda_{bulk})$

$T > T_{liq.}$: $\lambda_{eff.} \equiv \lambda_{massive}$

where λ_{bulk} is the thermal conductivity of the powder bed at room temperature. From measurements, it was found that λ_{bulk} is immeasurable small. For the calculations it was generally set to λ_{bulk} = 1W/mK.

3.3 Chemical submodel

Laser sintering of metal powders would be impossible, if oxydation would not be prevented or limited by, for example, protective atmosphere. The purity of the gas atmosphere within the process chamber is important, especially when producing clean or super clean metal. Oxygen, the most critical element in terms of undesirable reactions, can be present either in the gas atmosphere, as humidity or moisture in the powder or from oxyde layers on the powder particles. In order to get an idea of maximum allowable O_2-partial pressures, an Richardson-Ellingham diagramme can be considered [14]. When chemical reactions can be controlled or at least avoided as far as possible, the variety of SLS materials can be widened. This is important in particular at compound powders (like hard metals), where wetting is the decisive bonding mechanism. Furthermore the quality of the structure as well as the material properties rise.

3.4 Metallurgical submodel

The metallurgical submodel might seem to be of secondary importance. But changes in the state of aggregation, especially semisolid conditions, were identified to be an essential for the fusion behaviour, as was already mentioned above. Alloying mechanisms are of high interest when processing metal-metal powder mixtures instead of using alloy powders.

Also lattice energies, which are counted among metallurgy, should be considered in the energy balance of the thermal submodel in order to ensure a sufficient accuracy of the simulation results. The amount of the lattice energy can easily exceed the energy amount necessary for a temperature increase of 500 °C [14].

Last but not least, metallurgical processes influence strongly the mechanical properties of the resulting SLS part. Metallurgical mechanisms can be explained and controlled by the history of the temperature field (heating and cooling rates). Conclusions can be drawn for the design of an appropriate process strategy. Metallurgy has to be treated for each alloy individually; examples can be found in [2], for instance.

3.5 Sintering submodel

The Sintering submodel includes effects that refer to material transport. The SLS process can be regarded as short time liquid state sintering. Therefore solid state sintering effects, such as diffusion mechanisms, have not been considered up to now. The sintering in liquid phases depends on surface tension and viscosity [15]. As mentioned above, investigations indicated, that semisolid conditions of metal melts are advantageous to avoid bead formation and getting a dense sintering structure instead [13]. However, it was concluded from the investigations that the dependence of the relative density from temperature can be formulated approximately as follows:

$$\rho_{rel.}(T) = \frac{(T_{liq.} - T)}{(T_{liq.} - T_{sol.})} (\rho_{massive} - \rho_{bulk}) + \rho_{bulk}$$

where $\rho_{massive}$ is the compact density of the material and ρ_{bulk} is the bulk density of the powder bed.

4 SIMULATION

On the base of the submodelling, a computer simulation of the process was performed by Finite Elements Method (FEM). All submodels, except the chemical submodel, were included here: the optical submodel for the definition of the heat source; the thermal and the sintering submodel to calculate the output variables T and $\rho_{rel.}$ respectively the geometric shrinkage. The

metallurgical process of melting was considered by including the heat of fusion.

The principle of the FEM model and the boundary conditions of the FEM model are shown in figure 4. Subject of the simulation was a single laser pulse, occurring from above (positive z-direction). In real SLS, the laser beam is travelling along a line on the powder bed surface. Nevertheless, the laser pulse simulation can be used to draw conclusions on the results of line scanning: from the exposure times $t_{exp.}$, the referring scanning velocities v can roughly be calculated by the relation $v = d_B/t_{exp.}$, where d_B is the laser beam focus diameter. The advantage of a pulse simulation is a much shorter data processing time.

The geometry of the FEM model represents one powder layer (thickness 50 µm) situated on a sintered structure (cube of 1 mm³), see figure 4. The corner of the cube is radiated with a laser beam pulse (quarter circle) of the power P for the exposure time $t_{exp.}$. Originally, the laser beam has a round shape (focus diameter d_B = 0,5 mm) and gaussian intensity distribution. In the calculations, the laser power P and exposure time $t_{exp.}$ have been varied. In figure 5, the results for the material Inconel 718 are shown. Three different parameter sets S have been varied, i.e. S_1 [P = 200 W, $t_{exp.}$ = 5,9 ms], S_2 [P = 170 W, $t_{exp.}$ = 10 ms] and S_3 [P = 125 W, $t_{exp.}$ = 50 ms].

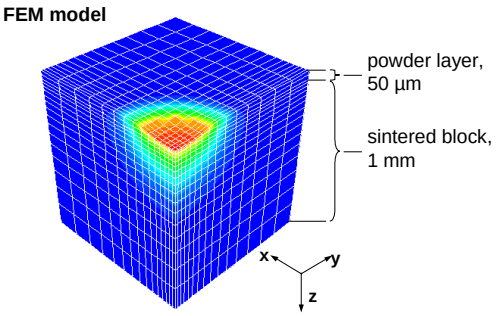

Boundary conditions

Heat source:
– CO_2 laser, 0 - 200 W
– beam diameter 0,5 mm
– gaussian energy distribution
– volumetric heat source

Powder material properties:
– $c_p = f(\rho_{rel.}, T)$
– $\lambda = f(\rho_{rel.}, T)$
– shrinkage $= f(\rho_{rel.})$
– $\rho_{rel.} = f(T)$
– H_{melt} = 289 J/g
– $T_{sol.}$ = 1300 °C
– $T_{liq.}$ = 1365 °C

Sintered (massive) material properties:
– $c_p = f(T)$
– $\lambda = f(T)$
– ρ = 8,5 g/cm³
– H_{melt} = 289 J/g
– $T_{sol.}$ = 1300 °C
– $T_{liq.}$ = 1365 °C

Figure 4: FEM model and boundary conditions of the SLS process simulation.

The objective of the process simulation was to determine the sintering depths, respectively the positions of the liquidus and solidus isotherms. Also the area of semisolid material within the heat-affected zone was identified.

5 DISCUSSION AND CONCLUSION

The underlying base of the integrated process model is the process analysis. The parameters mentioned here refer from experience of the past. Supplementation may be warranted and will be possible, when research provides further insight.

The description of the submodels made here are primary approaches. Refinements will have to be done, as soon as more investigation results of theoretical and practical kind will be available. However, the submodels all have an impact on the final result of SLS: either they "consume" or "contribute" energy to the overall energy balance or they cause forces influencing the process (coalescence and wetting).

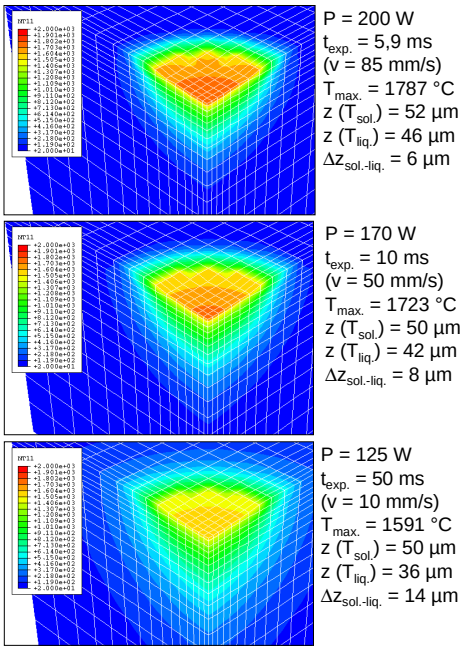

Figure 5: Simulation results of the laser pulse scanning; material: Inconel 718.

By combining submodels, specific mechanisms of relevance can be simulated. Up to now, only two field parameters, i.e. temperature and relative density, have been implemented. Thus the propagation of temperature fields and geometric shrinkage have been simulated. But also processes of nucleation, alloying or oxydation are possible to simulate, if more knowledge about these sub mechanisms will be available.

The FEM model was applied to the nickel base alloy Inconel 718, but can also be used to perform simulation on other metal powders. The temperature fields, shown in figure 5, indicate that low laser powers and long exposure times lead to expanded semisolid areas. The semisolid state is advantageous for SLS, as was supported by practical tests on SLS parameter sets [2]. Facing this, the conclusion was drawn, that materials with expanded solid-liquid temperature ranges are well suited for SLS. The smaller the semisolid temperature range of an alloy is, the lower the scanning velocity v and the laser power P have to be.

6 SUMMARY

The presented integrated model of SLS was developed on the base of an intense process analysis. From experience and examinations in the past, five sub-processes have been identified that make the nature of metal laser sintering, e.g. the optical, the thermal, the chemical, the metallurgical and the sintering process. Each sub-process has its own physical laws, which can be described separately, but also, the sub-processes are effecting each other continuously during the real SLS process. Therefore, a numerical calculation is well suited to simulate the interaction of all sub processes. Results of a combined temperature-shrinkage FEM analysis of laser sintering of the nickel base alloy Inconel 718 were presented. The objective of the laser pulse simulation performed here, was the determination of liquid, solid and semisolid states in the powder bed. The result was

helpful to optimize process parameters in order to enhance the technical quality of SLS parts.

7 REFERENCES

[1] Sun, M-S. M., 1991, Physical Modeling of the Selective Laser Sintering Process, Dissertation University of Texas, Austin/Texas.

[2] Wagner, C., 2003, Untersuchungen zum Selektiven Lasersintern von Metallen, Dissertation RWTH Aachen/Germany.

[3] Over, C. et al., 2001, Selective Laser Melting: A new approach for the direct Manufacturing of Metal Parts and Tools, Proceedings of the LANE International Conference, Erlangen/Germany.

[4] Wohlert, M.S., 2000, Hot Isostatic Pressing of Direct Selective Laser Sintered Metal Components, PhD Dissertation, University of Texas, Austin/Texas.

[5] Cantello, M., Ricciardi, G., Gobbi, S.L., 1996, Laser Welding of Superalloys for the Manufacturing of Aeroengine Components, Annals of the CIRP, 46/1:173-178.

[6] Glardon, R., Karapatis, N., Romano, V., 2001, Influence of Nd:YAG Parameters of the Selective Laser Sintering of Metallic Powders, Annals of the CIRP, 50/1:133-136

[7] O´Neil, W, Sutcliffe, C.J., Morgan, R., Landsborough, A., Hon, K.K.B., 1999, Investigation on Multi-Layer Direct Metal Laser Sintering of 316L Stainless Steel Powder Beds, Annals of the CIRP, 48/1:151-154

[8] Kurita, T., Morita, N., 1998, Basic Investigation on Laser Processing, 12th International Symposium for Electromachining ISEM, Aachen/Germany, 585-592.

[9] Kruth, J.P., Wang, X., Laoui, T., Froyen, L., Progress in Selective Laser Sintering, 13th International Symposium for Electromachining ISEM, Bilbao/Spain, 21-38.

[10] Beyer, E., Wissenbach, K., 1998, Oberflaechenbehandlung mit Laserstrahlung, Springer Verlag, Berlin-Heidelberg-New York.

[11] Gasser, A., 1993, Oberflaechenbehandlung metallischer Stoffe mit CO_2-Laserstrahlung in der fluessigen Phase, Dissertation RWTH Aachen/Germany.

[12] Schluender, E.-U., Tsotsas, E., 1988, Waermeuebertragung in Festbetten, durchmischten Schuettguetern und Wirbelschichten, Georg Thieme Verlag, Stuttgart-New York.

[13] Klocke, F., Wagner, C., 2003, Coalescence Behaviour of Two Metallic Particles as Base Mechanism of Selective Laser Sintering, to be published in: Annals of the CIRP, 52/1.

[14] Frohberg, M., 1994, Thermodynamik fuer Werkstoffingenieure und Metallurgen, Deutscher Verlag fuer Grundstoffindustrie, Leipzig-Stuttgart.

[15] Frenkel, J., 1945, Viscous Flow of Crystalline Bodies under the Action of Surface Tension. Journal of Physics, Moscow, Vol. 9 Nr. 5: 385-391.